Asian Journal of Chemistry; Vol. 32, No. 9 (2020), 2381-2388

ASIAN JOURNAL OF CHEMISTRY

https://doi.org/10.14233/ajchem.2020.22481

Evaluation of Mg/Al Layered Double Hydroxides as Adsorbent Material for Adsorptive Removal of Congo Red (Acid Red 28) Azodye from Aqueous Solution

LAM VAN TAN[1,*], HONG THAM NGUYEN THI[1,2], TO UYEN DAO THI[3] and VAN THUAN TRAN[1,2,*]

[1]NTT Hi-Tech Institute, Nguyen Tat Thanh University, Ho Chi Minh City, Vietnam
[2]Center of Excellence for Green Energy and Environmental Nanomaterials, Nguyen Tat Thanh University, Ho Chi Minh City, Vietnam
[3]Center of Excellence for Functional Polymers and NanoEngineering, Nguyen Tat Thanh University, Ho Chi Minh City, Vietnam

*Corresponding author: E-mail: lvtan@ntt.edu.vn

Received: 5 October 2019; *Accepted*: 25 July 2020; *Published online*: 20 August 2020; AJC-20042

The use of inorganic layer compounds as adsorbents for organic dyes in water treatment is of increasing interest. In this study, an attempt is made for the synthesis of Mg/Al LDHs by the hydrothermal method. The synthesis temperature was found to significantly affect to the structure of layered double hydroxides (LDHs), as pointed out by FT-IR analysis. In addition, an adsorption capacity of the synthesized LDHs against Congo red in aqueous solutions was investigated and also compared the adsorption results with other dyes such as methylene blue and methyl orange.

Keywords: Inorganic layer compounds, Adsorption, Congo red, Isotherms.

INTRODUCTION

Congo red have been recognized as a group of organic compounds which have good capability of inhibiting metal corrosion due to the presence of 4-amino-1-naphthalene-sulphonic acid groups located at the end of two azo bonds [1,2]. However, the stability of the aromatic structure brings about serious pollution environment. In order to remedy the issue, various approaches have been proposed such as the use of activated carbon as an adsorbent or biological treatments [3-8]. However, the use of such methods, albeit simple and economical, is unable to degrade toxic and resistant organic pollutants. Among the possible techniques for water treatments, the solid adsorbents for adsorption process is one of the most efficient method due to simple design and low manufacturing cost.

Recent developments in material science related to its chemistry, physics and biology has enabled the synthesis of materials with novel properties and excellent performance [9-15]. Among them, porous materials have been recognized as a potential candidate in many applications such as adsorption, catalysis and energy storage [16-19]. Especially, layered double hydroxides (LDHs), due to highly tunable properties and the flexible exchange ion capacity in their structures, figure prominently in manufacture of absorbents. LDHs are commonly represented by the general formula of $[M^{2+}_{1-x}M^{3+}_{x}(OH)_2]^{x+}(A^{n-})_{x/n}\cdot mH_2O$, wherein, x equals to $M^{3+}/(M^{2+}+M^{3+})$ and A^{n-} is any intercalated anion. Apart from octahedrally coordinating Mg^{2+} ions by hydroxyl groups, isomorphous replacement of a fraction of Mg^{2+} ions with a trivalent cation, such as Al^{3+}, could also generate a positive charge on the layers. This feature allows for enlarging of surface areas and pore volume which facilitate adsorption processes [20-23].

Co-precipitation method has been the popular method in synthesis of LDHs. One notable attempt utilizing this technique was the synthesis of Mg/Al LDHs [24]. However, major drawbacks of the co-precipitation is the agglomeration and size-randomness of particles. In this context, we reported a simple method to synthesize Mg/Al LDHs by hydrothermal reaction at the different temperatures. The advantages of this method is the high crystallinity, low impurity content and stable crystal structure of the synthesized LHDs [25]. Since the crystal structure and phase transitions of the synthesized LHDs strongly depend on synthesis temperature, it is required to determine proper parameters of the hydrothermal process to achieve optimal adsorption capacity.

Herein, a new method used to synthesize Mg/Al LDHs was attempted and investigated with respect to different temperatures, hydrothermal urea method. The LDHs characteristics and capacity of adsorption against Congo red were also discussed in this study.

EXPERIMENTAL

$MgCl_2{\cdot}6H_2O$ (98%), $AlCl_3{\cdot}6H_2O$ (97%) and urea (99%), were purchased from Sigma Aldrich. Mg/Al LDHs were synthesized *via* hydrothermal method as follows. Initially, a mixture containing $AlCl_3{\cdot}6H_2O$ (8 mmol), $MgCl_2{\cdot}6H_2O$ (4 mmol), urea (128 mmol) and 60 mL of distilled water was magnetically stired at for 15 min. Then, this mixture was transferred into a 100 mL Teflon-lined autoclave and heated at 100, 150, 180 °C for 24 h in an oven. Finally, the obtained precipitate (white powder) was collected by centrifugation at 5000 rpm for 10 min, washed with deionized water and ethanol several times and then dried at 110 °C for 12 h and used for further studies.

Adsorption experiments: Adsorption experiments were performed by mixing 0.04 g Mg/Al LDHs with 100 mL of Congo red in a 150 mL beaker. The equilibrium adsorption capacity, q_e (mg/g), was calculated using following eqn:

$$q_e = \frac{(C_o - C_e)}{m} V$$

where C is the concentration of Congo red. M is the mass of Congo red. V is the volume of the dye solution (L). The subscript o and e denote initial and equilibrium states respectively.

Effect of Congo red concentration and contact time on adsorption capacity of the synthesized Mg/Al LDHs: Initially, 0.04 g of the adsorbent was transferred to 100 mL of dye solution. To determine the effect of the initial dye concentration and contact time for the removal of Congo red, the experiments were performed at 25 °C at varying initial concentrations from 20-50 mg/L and time periods from for 5 from 210 min. Before commencement and upon completion of each adsorption experiment, the supernatant solution was measured for Congo red concentration using a Tomos V-1100 UV/Vis spectrophoto-meter at 500 nm.

RESULTS AND DISCUSSION

Fourier transform infrared spectroscopy (FT-IR) results: The FT-IR spectra of samples synthesized at different temperatures are presented in Fig. 1. Typically, the strong and board bands in the range of 3525-3474 cm^{-1} are due to the streaching of O-H groups with the interlayer water molecules and hydrogen bonding [26]. Clearly, the intensity of this band heavily decreased at 180 °C. Around 1350 cm^{-1}, the absorption peaks were visually detected, suggesting the asymmetric stretching bond of intercalated Cl^-. The band at 634 and 773 cm^{-1} is possibly index to Al–OH stret-ching. The lattice vibration of metal–oxygen bonds (M–O) is indexed to absorption peaks located in 770-550 cm^{-1} region. Interestingly, it is found that stretching vibrations of Al–O bonding of γ-Al_2O_3 were associated with two characteristic peaks at 643.47 cm^{-1} and 738.60 cm^{-1}. This is consistent with a previous study [27] where elevated

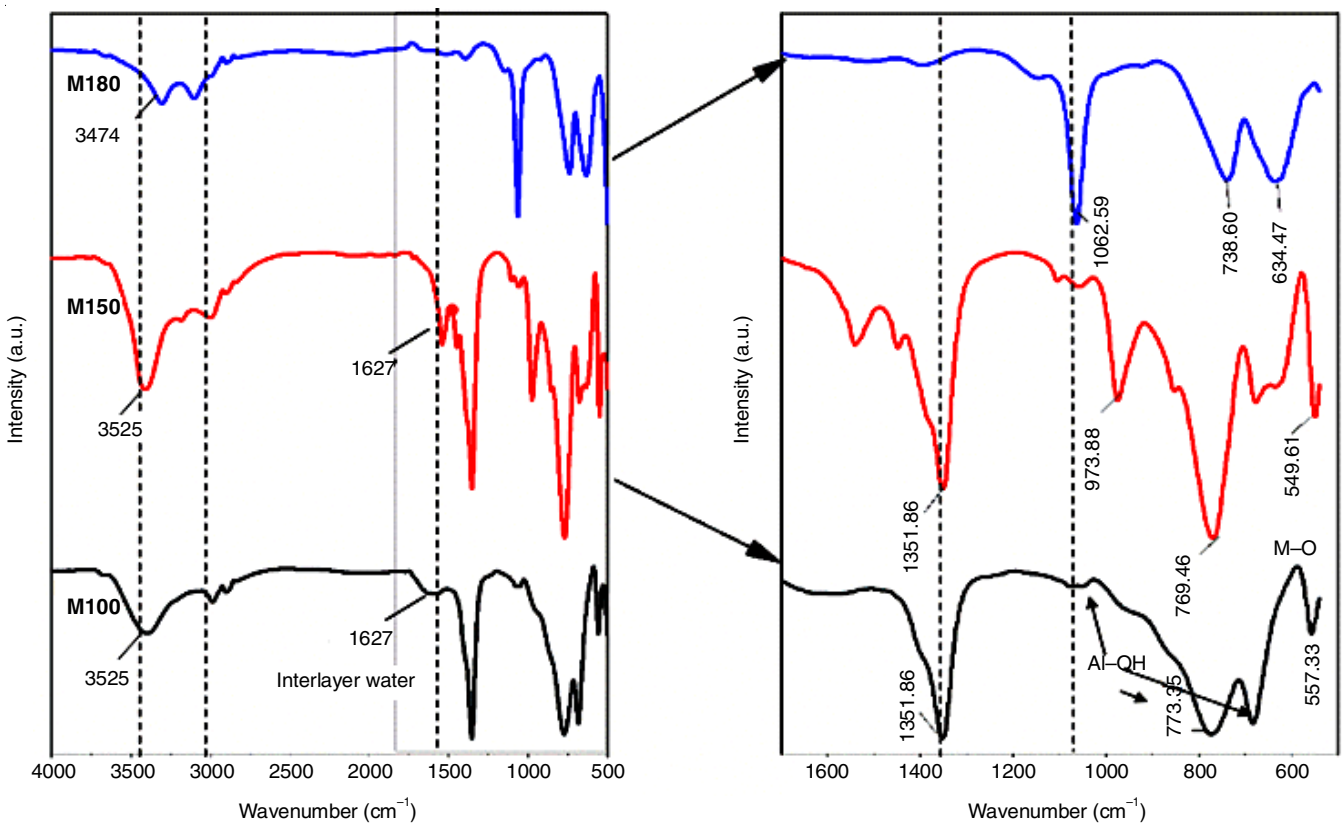

Fig. 1. FT-IR spectra of MgAl LDHs at 100, 150 and 180 °C

synthesis temperature was found to be associated with total decomposition of the interlayers LDHs and water molecules and, consequently, complete structural destruction of LHDs [28].

Effect of contact time and concentrations: Congo red adsorption onto LDHs with respect to varying contact time and Congo red concentrations was shown in Fig. 2. At first glance, the relationship between equilibrium time and Congo red adsorption was observed to be positive and two adsorption phases were also clearly defined. While in the first phase, which is within the first 50 min, rapid increase in adsorption capacity was attained due to the rapid surface adsorption, the second phase in the last 150 min only witnessed a small improvement of adsorption [29]. While the first phase could be explained by the abundance of unoccupied surface locations available for adsorption, the second phase is justified by insufficient active sites on the surface of LDHs, which in turn hinders surface interaction between Congo red molecules and LDHs. In absence of surface active sites, dye molecules move into the interlayer cavities of LDHs, eventually halting the adsorption process.

With regard to initial concentration, with the exception of the sample synthesized at 180 °C, all other samples exhibited the removal rate of dye that is highly dependent on the initial concentration of the solution. Specifically, peak removal rate was 54.961% and 54.093% at Congo red concentration of 20 ppm, respectively achieved for samples synthesized at 100 and 150 °C.

Adsorption kinetics: Investigation of adsorption kinetics is an important step in elaborating the adsorption mechanism and in evaluating removal efficiency of an adsorbent. In this study, the adsorption kinetics were investigated with regard to the pseudo-first-order and pseudo-second-order models. The experimental data were fitted with the two models to and determine the adsorption kinetics.

The Lagergren pseudo-first-order model incorporating solid capacity is given as.

$$\ln (q_e - q_t) = \ln (q_e) - k_1 t \quad (2)$$

where q (mg/g) is the quantity of solute adsorbed per gram of adsorbent, subscript e and t denote equilibrium state and at t time. k_1 (1/min) is the rate constant.

The pseudo second kinetics based on the assumption that two surface sites are involved in the adsorption process. To be specific, the expression of the model is presented as follows:

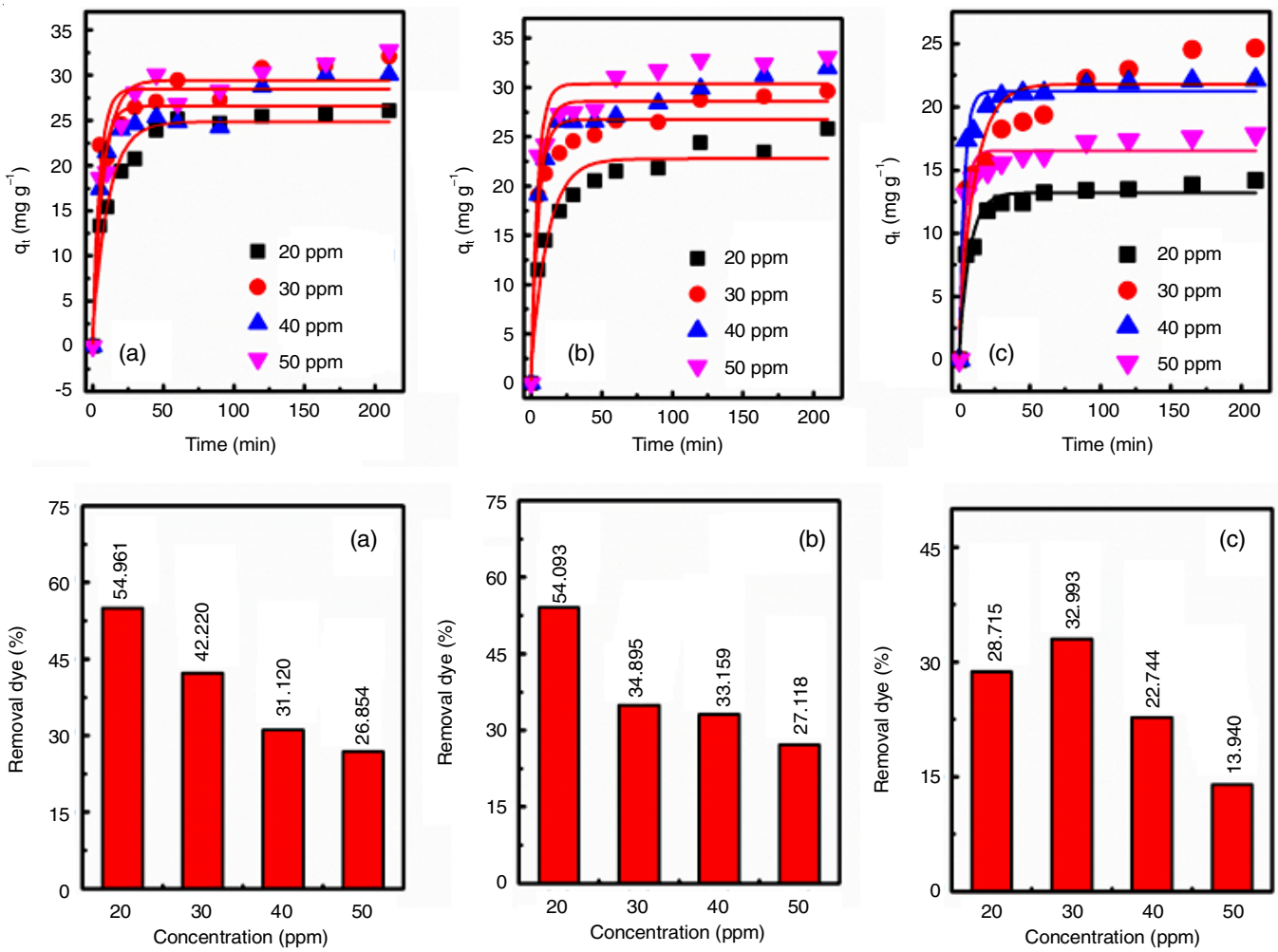

Fig. 2. Effect of concentrations of Congo red adsorption onto Mg/Al LDHs (a) 100 °C, (b) 150 °C, (c) 180 °C

$$\frac{dq}{dt} = K_2(q_e - q)^2$$

$$\frac{t}{q_t} = \frac{1}{k_2 q_e^2} + \frac{t}{q_e} \quad (3)$$

where k_2 (g/mg min) is the rate constant of pseudo-second order adsorption kinetics.

Non-linear regression was employed to approximate model parameters of the two kinetics. The obtained parameters and coefficients of determination are listed in Table-1. It is evident from Table-1 that, in comparison with the pseudo-first-order model (Fig. 3), the pseudo-second-order kinetic (Fig. 4) achieved a larger coefficient R^2 and had q_e values that are closer with the experimental values. This suggests that the adsorption of Congo red onto LDHs adhered to pseudo-second-order kinetics and that the chemsorption could be the factor that limits the rate of adsorption.

In order to model the heterogeneous diffusion process of gas adsorption, the Elovich model was adopted (Fig. 5). The model relates the quantity of solute adsorbed per gram of adsorbent at time t to the adsorption rate α (mg/g min) and the constant of desorption β (g/mg) as follows.

$$q_t = \frac{1}{\beta}\cdot\ln(\alpha.\beta) + \frac{1}{\beta}\cdot\ln(t)$$

The last employed model is the Bangham equation that describe the intra-particle diffusion mechanism at room temperature. The results revealed that for both adsorbents, the constant, α, increased in value while k_o value decreased as temperature was increased (Fig. 6). The linearity of the lines measured by R^2, which show that the R^2 values increases as indicating that diffusion of Cr(VI) into pores became less important in the rate determining step as temperature was increased. This may be attributed to the higher surface adsorption which increases adsorption kinetics by reducing diffusion paths within the adsorbent:

$$\log\log\left(\frac{C_o}{C_o - q_t\cdot\frac{m}{V}}\right) = \log\left(\frac{k_B}{2.303.V}\right) + \alpha_B.\log\ (t)$$

Adsorption isotherm: To shed light into the interaction between solutes and adsorbents and optimize adsorbent dosage, approximation of different isotherm models using adsorption

TABLE-1
KINETICS MODEL PARAMETERS FOR ADSORPTION OF CONGO RED USING Mg/Al LDHs

Kinetic models	Parameters	Unit	Value		
			100 °C	150 °C	180 °C
Pseudo first-order	k_1	$min^{-1}/(mg/L)^{1/n}$	0.0123	0.0208	0.0147
	$q_{e,exp}$	mg/g	32.7581	33.0892	17.8428
	$q_{e,cal}$	mg/g	10.4925	9.6135	3.4441
	R^2	–	0.7127	0.8146	0.5688
Pseudo second-order	$q_{e,exp}$	mg/g	32.7581	33.0892	17.8428
	$q_{e,cal}$	mg/g	33.0142	33.7154	17.9565
	$H = k_2.q_e^2$	–	4.2242	6.4321	3.6220
	R^2	–	0.9955	0.9989	0.9935
Elovich	β	g/mg	0.258	0.3447	0.785
	α	mg/(g.min)	92.07	1476.45	8251.75
	R^2	–	0.98121	0.97583	0.99278
Bangham	α_B	–	0.17437	0.1184	0.0875
	R^2	–	0.93653	0.95468	0.97938
	K_B	mL/(g/L)	0.0127	0.01725	0.00955

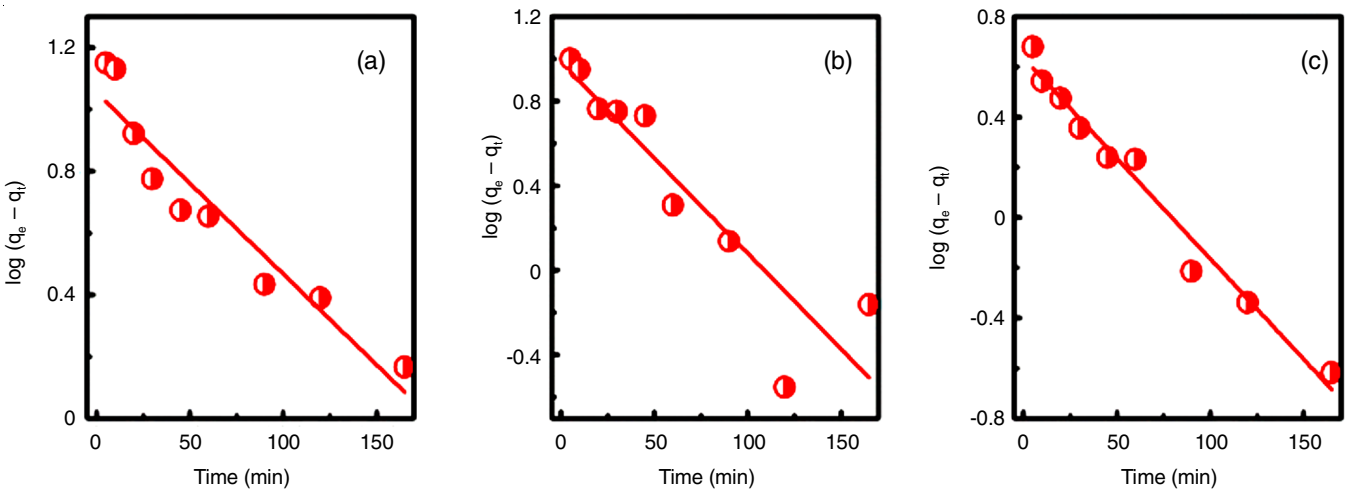

Fig. 3. Pseudo-first-order kinetic plots for adsorption of Congo red using Mg/Al LDHs: (a) 100 °C, (b) 150 °C, (c) 180 °C

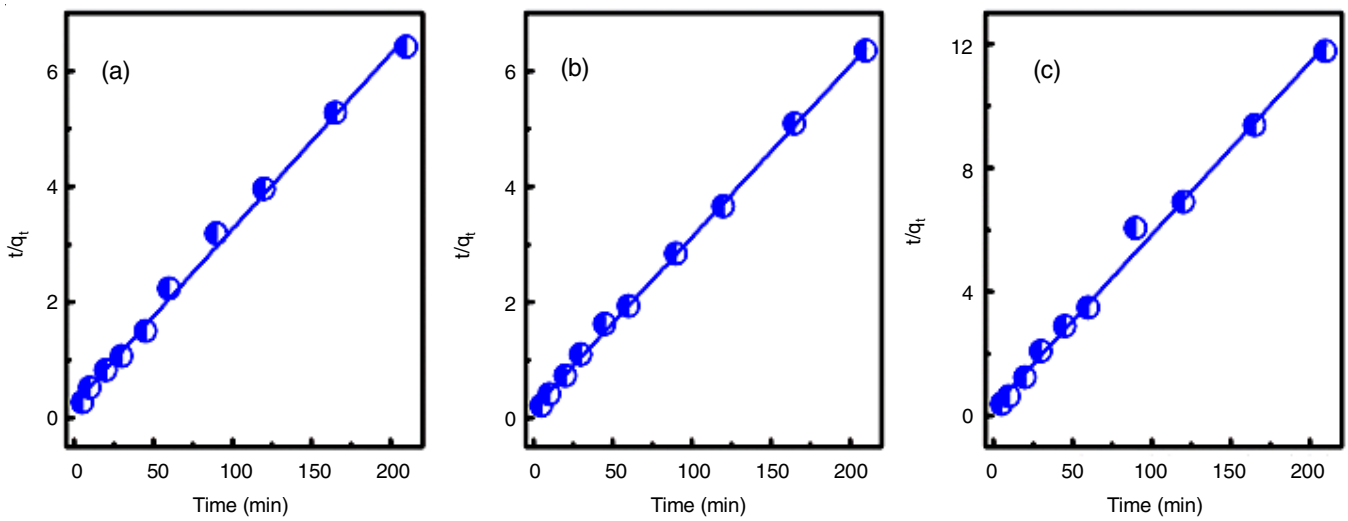

Fig. 4. Pseudo-second-order kinetic plots for adsorption of Congo red using Mg/Al LDHs: (a) 100 °C, (b) 150 °C, (c) 180 °C

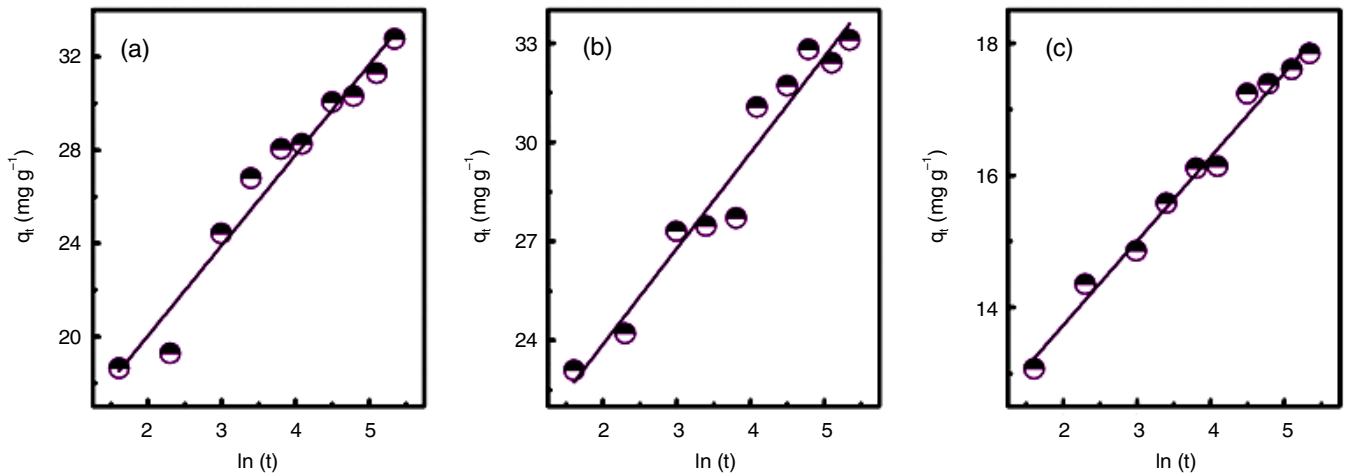

Fig. 5. Elovich kinetic plots for adsorption of Congo red using Mg/Al LDHs: (a) 100 °C, (b) 150 °C, (c) 180 °C

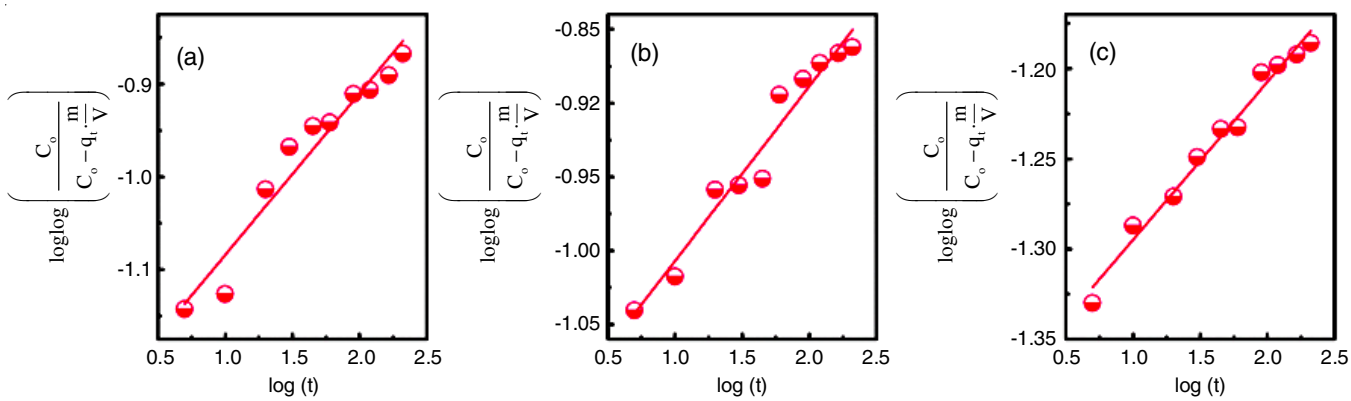

Fig. 6. Bangham kinetic plots for adsorption of Congo red using Mg/Al LDHs: (a) 100 °C, (b) 150 °C, (c) 180 °C

equilibrium data was performed. Four adsorption isotherms including Langmuir, Freundlich, Temkin and Dubinin-Radushkevich were utilized and the most suitable model was determined using the coefficient of determination (R^2).

The first isotherm, the Langmuir adsorption model, which describes the monolayer adsorption onto a surface having finite identical sites is shown as follows:

$$\frac{C_e}{q_e} = \frac{1}{bq_m} + \frac{C_e}{q_m} \quad (4)$$

where q_e (mg/g) and C_e (mg/L) are defined as equilibrium concentration of adsorbate, respectively in the adsorbent- and aqueous-phase, q_m (mg/g) and b (L/mg) is the maximum sorption capacity and the Langmuir constant, respectively.

The favourability of the adsorption isotherm could be assessed through the equilibrium parameter, R_L, which is defined by eqn. 5 as follows:

$$R_L = \frac{1}{1 + bC_o} \quad (5)$$

where C_o is highest initial dye concentration. Depending on the value of the parameter, the isotherm could be either irreversible ($R_L = 0$), favourable ($0 < R_L < 1$), linear ($R_L = 1$) or unfavourable ($R_L > 1$). Parameter results from the Table-2 imply that, except for the sample synthesized at 180 °C, the Congo red adsorption process onto Mg/Al LDHs was favourable.

The second isotherm, the Freundlich model assumes that the surface of the adsorbent was heterogeneous and that different adsorption energies occurred and were dependent on surface coverage. The model is expressed as follows:

The empirical Freundlich model which is known to be adequate for low concentrations is expressed by the following equation:

$$\log (q_e) = \frac{1}{n} \log (C_e) + \log k \quad (6)$$

where q_e (mg/g) and C_e(mg/L) are defined similarly to the Langmuir adsorption model. k and n are Freundlich constants which are related to adsorption capacity and adsorption intensity. Approximation results for k, 1/n, q_m, b and the correlation coefficients for the two isotherms were presented in Table-2.

The third isotherm, the Temkin model, accommodates the interaction between adsorbent and adsorbate by including a separate parameter. The model neglects outlying concentrations and assumes the linear, inverse, rather than logarithmic, relationship between heat of adsorption (function of temperature) of all molecules in the layer and coverage. The derivation of the model featured the binding energies in the form of a uniform distribution function. The slope and the intercept of the model are obtained by approximating the data of the quantity sorbed q_e and ln C_e. Model constants were determined from the estimated slope and intercept.

$$q_e = \frac{RT}{b} \ln(A_T C_e)$$

$$q_e = \frac{RT}{b_T} \ln(A_T) + \ln(C_e)$$

$$B = \frac{RT}{b}$$

$$q_e = B \ln (A_T) + B \ln C_e$$

where, A_T = Temkin isotherm equilibrum bingding constant (L/g); b_T = Temkin isotherm constant; R = universal gas constant (8.314 J/mol/K); T = Temperature at 298 K; B = Constant related to heat of sorption (J/mol).

The third isotherm, the Dubinin-Radushkevich model, was adopted to elaborate the adsorption mechanism that has Gaussian energy distribution onto a heterogeneous surface. Advantages of the model was the capability of approximating high solute activities and a good concentration range.

$$q_e = (q_s)_{exp} - (K_{ad}\varepsilon^2)$$

$$\ln q_e = \ln q_s - (K_{ad}\varepsilon^2)$$

where q_e = amount of absorbate in the adsorbent at equilibrium (mg/g); Q_s = Theoretical isotherm saturation capacity (mg/g); K_{ad} = Dubinin-Radushkevich isotherm constant (mol^2/kJ^2); ε = Dubinin-Radushkevich isotherm constant.

In this model, adsorption of metal ions is separated with mean free energy. Per each molecule, E required to translocate from its location in the sorption space to the infinity could be expressed as follows.

$$E = \left(\frac{1}{\sqrt{2K_{ad}}} \right)$$

where the K_{ad} could be obtained from the isotherm equation. The can be calculated as:

$$\varepsilon = RT \ln \left(1 + \frac{1}{C_e} \right)$$

where R, T and C_e represent the gas constant (8.314 J/mol K), absolute temperature (K) and adsorbate equilibrium concentration (mg/L), respectively.

It could be concluded from the coefficient of determination (R^2) in Table-2 (Fig. 7) that the Freundlich isotherm is the most appropriate model to describe the adsorption process of the material synthesized at 100 °C. For samples synthesized at 150 and 180 °C, the Langmuir model was the model that best described the experimental data.

Applicability with other dyes removal: Similar adsorption experiments onto Mg/Al LDHs were performed with

TABLE-2
PARAMETERS OF LANGMUIR, FREUNDLICH, TEMKIN AND DUBININ-RADUSHKEVICH ISOTHERMS FOR ADSORPTION OF DYES ONTO Mg/Al LDHs

Sample	Langmuir				Freundlich			
	q_e (mg/g)	b (L/mg)	R_L	R^2	1/n	n	k_F (mg/g)	R^2
100 °C	48.685	0.103	0.162	0.981	0.336	2.976	11.709	0.990
150 °C	50.659	0.094	0.175	0.927	0.329	3.034	12.058	0.862
180 °C	18.786	-1.644	-0.012	0.825	0.140	7.143	12.289	-0.379
Sample	Temkin				Dubinin-Radushkevich			
	A_T (L/mg)	b_T	B	R^2	q_s (mg/g)	K_{ad} (mol^2/kJ^2)	E (KJ/mol)	R^2
100 °C	0.769	168.165	14.733	0.969	461.518	$3.891.10^{-5}$	113.358	0.913
150 °C	1.389	237.020	10.453	0.828	388.506	$3.628.10^{-5}$	117.395	0.696
180 °C	1.025	1241.891	1.995	-0.432	267.730	$3.929.10^{-5}$	112.809	-0.215

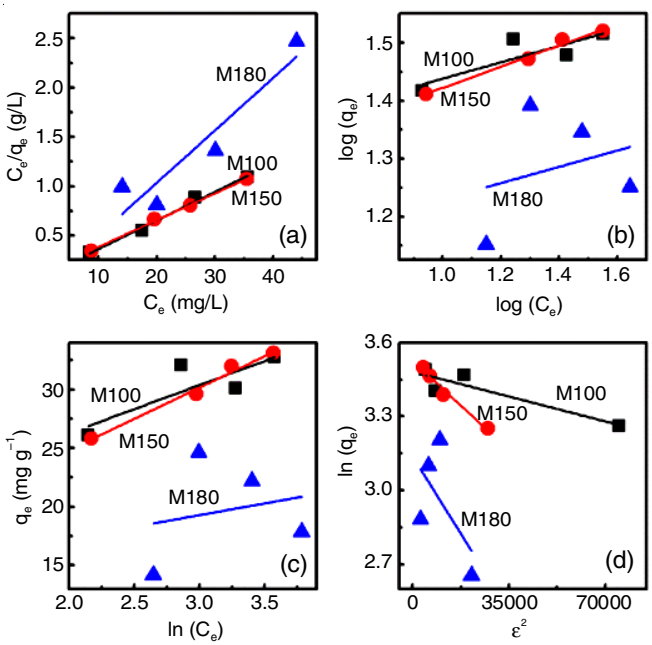

Fig. 7. Isotherm models of Mg/Al LDHs: (a) Langmuir isotherm model; (b) Freundlich isotherm model; (c) Temkin isotherm model; (d) Dubinin-Radushkevich isotherm model

methylene blue and methyl orange dyes also. In this experiment, synthesized Mg/Al LDHs at 100 °C was used. Material mass and contact time were fixed at 0.04 g and 90 min, respectively. Fig. 8 illustrated maximum adsorptions of the material against various tested dyes (Congo red, methyl orange, methylene blue). When compared with the adsorption capacity onto Mg/Al LDHs towards the different dyes such as Congo red, methyl orange and methylene blue, it is easily observed that Mg/Al LDHs achieved the highest adsorption capacity towards Congo red. This is possibly due to a large number of positively charged functional groups existing on the surface Mg/Al LDHs, facilitating the adsorption of anionic dyes such as Congo red or methyl orange. Herein, capacity of adsorption of Congo red was higher than that of methyl orange due to the structural difference between the two dyes. These featured indicate that Mg/Al LDHs is a promising material for adsorption of anionic dyes in industrial discharges.

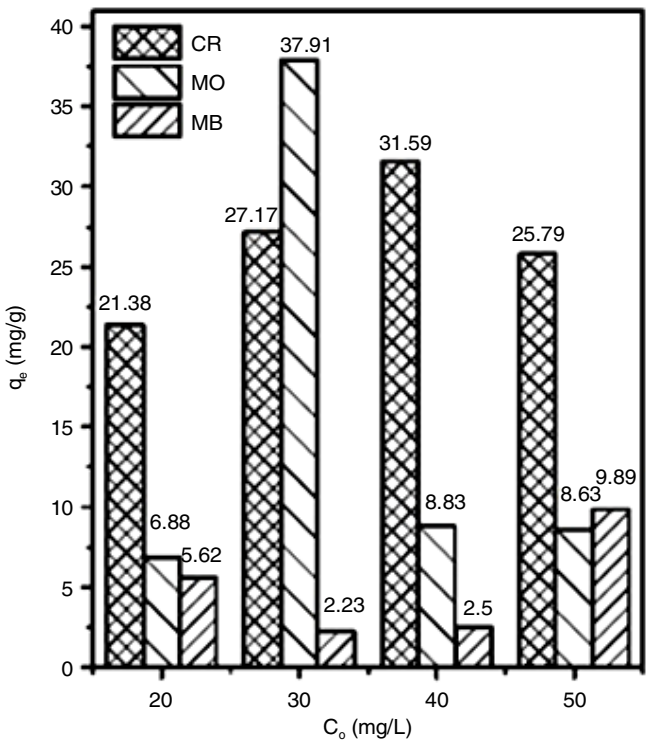

Fig. 8. Comparison of adsorption capacity of Mg/Al LDHs against three dyes (CR = Congo red; MO= methyl orange; MB = methylene blue)

Performance evaluation: To prove that the current adsorbent is better for the removal of Congo red, the maximum adsorption capacity (q_m) of Mg/Al LDHs with the previous literature [30-35], which calculated from Langmuir isotherm model, are presented in Table-3. All of the adsorbents used for removing Congo red have significantly lower q_m values than Mg/Al LDHs used in this report. The environmental concern with regard to discharges contaminated with toxic organic dyes could be handled by a current potential material (Mg/Al LDHs).

TABLE-3
COMPARISON OF MAXIMUM ADSORPTION CAPACITY (q_m) VALUES OBTAINED FROM VARIOUS ABSORBENTS TOWARDS THE REMOVAL OF CONGO RED DYE

Type of adsorbent	q_m (mg/g)	Ref.
Montmorillonite	12.70	[30]
Anilinepropylsilica xerogel	22.68	[31]
Coir pith	6.72	[32]
Bagasse fly ash	11.885	[33]
Activated red mud	7.08	[34]
Waste Fe(III)/Cr(III) hydroxide	44.00	[35]
Mg/Al LDHs	48.685	Present work

Conclusion

We have successfully synthesized Mg/Al LDHs from magnesium chloride and aluminum chloride *via* urea hydrolysis routine under hydrothermal conditions. The effects of thermal conditions on adsorption capacities against Congo red dye were investigated and adsorption mechanism was elaborated using multiple isotherms and kinetics. From the results, some conclusions can be drawn. First, it was found that the proper temperature for hydrothermal synthesis of Mg/Al LDHs was 100 °C. Second, the second pseudo-order kinetics and the Langmuir model were the models that best described the adsorption process and experimental data.

ACKNOWLEDGEMENTS

This study was supported by grants from Nguyen Tat Thanh University, Ho Chi Minh City, Vietnam.

CONFLICT OF INTEREST

The authors declare that there is no conflict of interests regarding the publication of this article.

REFERENCES

1. E.E. Oguzie, *Mater. Chem. Phys.*, **87**, 212 (2004); https://doi.org/10.1016/j.matchemphys.2004.06.006
2. V.T. Pham, H.-T. T. Nguyen, D. Thi Cam Nguyen, H. T. N. Le, T. Thi Nguyen, N. Thi Hong Le, K.T. Lim, T. Duy Nguyen, T.V. Tran and L.G. Bach, *Processes*, **7**, 305 (2019); https://doi.org/10.3390/pr7050305
3. D. Eeshwarasingh, P. Loganathan and S. Vigneswaran, Chemosphere, **223**, 616 (2019); https://doi.org/10.1016/j.chemosphere.2019.02.033
4. H. Xu, M.-X. Zhan, P.-T. Cai, L.-J. Ji, T. Chen and X.-D. Li, *Energy Fuels*, **33**, 11477 (2019); https://doi.org/10.1021/acs.energyfuels.9b02723
5. A.H.A. Khan, M. Ayaz, M. Arshad, S. Yousaf, M.A. Khan, M. Anees, A. Sultan, I. Nawaz and M. Iqbal, *Iran. J. Sci. Technol., Trans. A: Sci.*, **43**, 1393 (2019); https://doi.org/10.1007/s40995-017-0393-8
6. E. Shahsavari, A. Schwarz, A. Aburto-Medina and A.S. Ball, *Curr. Pollut. Rep*., **5**, 84 (2019); https://doi.org/10.1007/s40726-019-00113-8
7. H.-H. Li, Y.-T. Wang, Y. Wang, H.-X. Wang, K.K. Sun and Z.-M. Lu, *J. Zhejiang Univ. Sci. B*, **20**, 528 (2019); https://doi.org/10.1631/jzus.B1900165
8. M. Khadhraoui, H. Trabelsi, M. Ksibi, S. Bouguerra and B. Elleuch, *J. Hazard. Mater.*, **161**, 974 (2009); https://doi.org/10.1016/j.jhazmat.2008.04.060
9. L.M.T. Nguyen, J. Kim, B.L. Giang, T.M. Al Tahtamouni, P.T. Huong, C. Lee, N.M. Viet and D.Q. Trung, *J. Ind. Eng. Chem.*, **80**, 597 (2019); https://doi.org/10.1016/j.jiec.2019.08.037
10. V.H. Nguyen, Q.T.P. Bui, D.V.N. Vo, K.T. Lim, L.G. Bach, S.T. Do, T.V. Nguyen, V.D. Doan, T.D. Nguyen and T.D. Nguyen, *Materials*, **12**, 2681 (2019); https://doi.org/10.3390/ma12172681
11. C.N.R. Rao, S.R.C. Vivekchand, K. Biswasa and A. Govindaraja, *Dalton Trans*., 3728 (2007); https://doi.org/10.1039/B708342D
12. I. Khan, K. Saeed and I. Khan, *Arabian J. Chem*., **12**, 908 (2019); https://doi.org/10.1016/j.arabjc.2017.05.011
13. S. Xiong and L. Wang, *Adv. Mater. Sci. Eng*., **2020**, 5903457 (2020); https://doi.org/10.1155/2020/5903457
14. L.A. Dobrzanski, *J. Mater. Process. Technol*., **175**, 133 (2006); https://doi.org/10.1016/j.jmatprotec.2005.04.003
15. M.O. Steinhauser and S. Hiermaier, *Int. J. Mol. Sci*., **10**, 5135 (2019); https://doi.org/10.3390/ijms10125135
16. L.-Y. Wang, X.-H. Yu and Z. Zhao, *Acta Phys. Chim. Sin*., **33**, 2359 (2017); https://doi.org/10.3866/PKU.WHXB201706094
17. S. Rashidi and J.A. Esfahani and A. Rashidi, *Renew. Sustain. Energy Rev*.,, **73C**, 1198 (2017); https://doi.org/10.1016/j.rser.2017.02.028
18. H. Nakajima, *Mater. Trans*., **60**, 2481 (2019); https://doi.org/10.2320/matertrans.MT-M2019182
19. T. Jibowu, *Front. Nanosci. Nanotechnol*., **2**, 165 (2016); https://doi.org/10.15761/FNN.1000129
20. M.J. Sultana and F.R.S. Ahmed, *Am. J. Nanosci*., **4**, 16 (2018); https://doi.org/10.11648/j.ajn.20180402.11
21. K.K. Sadasivuni, J.-J. Cabibihan, K. Deshmukh, S. Goutham, M.K. Abubasha, J.P. Gogoi, I. Klemenoks, G. Sakale, B.S. Sekhar, P. S. Rama Sreekanth, K.V. Rao and M. Knite, *Polym.-Plast. Technol. Mater*., **58**, 1253 (2019); https://doi.org/10.1080/03602559.2018.1542729
22. M. Laipan, J. Yu, R. Zhu, J. Zhu, A.T. Smith, H. He, D. O'Hare and L. Sun, *Mater. Horiz*., **7**, 715 (2020); https://doi.org/10.1039/C9MH01494B
23. L.G. Bach, M.R. Islam, X.T. Cao, J.M. Park and K.T. Lim, *J. Alloys Mater.*, **582**, 22 (2014); https://doi.org/10.1016/j.jallcom.2013.07.186
24. N. Ayawei, S.S. Angaye, D. Wankasi and E.D. Dikio, *Open J. Phys. Chem. Synth.*, **5**, 56 (2015); https://doi.org/10.4236/ojpc.2015.53007
25. J. Wang, L.A. Stevens, T.C. Drage and J. Wood, *Chem. Eng. Sci.*, **68**, 424 (2012); https://doi.org/10.1016/j.ces.2011.09.052
26. C.H. Lin, H.L. Chu, W.S. Hwang, M.C. Wang and H.H. Ko, *AIP Adv.*, **7**, 125005 (2017); https://doi.org/10.1063/1.4990832
27. W.L. Li, S.B. Tian, and F. Zhu, *The Scientific World J.*, **2013**, 838374 (2013); https://doi.org/10.1155/2013/838374
28. G. Starukh, *Nanoscale Res. Lett.*, **12**, 391 (2017); https://doi.org/10.1186/s11671-017-2173-y
29. O.S. Bello and S. Banjo, *Toxicol. Environ. Chem.*, **94**, 1114 (2012); https://doi.org/10.1080/02772248.2012.691504
30. L. Wang and A. Wang, *J. Hazard. Mater.*, **147**, 979 (2007); https://doi.org/10.1016/j.jhazmat.2007.01.145
31. C. Namasivayam and D. Kavitha, *Dyes Pigments*, **54**, 47 (2002); https://doi.org/10.1016/S0143-7208(02)00025-6
32. F.A. Pavan, S.L.P. Dias, E.C. Lima and E.V. Benvenutti, *Dyes Pigments*, **76**, 64 (2008); https://doi.org/10.1016/j.dyepig.2006.08.027
33. I.D. Mall, V.C. Srivastava, N.K. Agarwal and I.M. Mishra, *Chemosphere*, **61**, 492 (2005); https://doi.org/10.1016/j.chemosphere.2005.03.065
34. A. Tor and Y. Cengeloglu, *J. Hazard. Mater.*, **138**, 409 (2006); https://doi.org/10.1016/j.jhazmat.2006.04.063
35. C. Namasivayam, R. Jeyakumar and R.T. Yamuna, *Waste Manag.*, **14**, 643 (1994); https://doi.org/10.1016/0956-053X(94)90036-1